Torque Characterization of Magnetorheological Brake using Finite Element Analysis

CHIRANJIT SARKAR[1] and HARISH HIRANI[2]
[1,2]Department of Mechanical Engineering
[1]Delhi Technological University
Bawana Road, Delhi -110042
[2]Indian Institute of Technology Delhi
Hauz Khas, New Delhi -110006
INDIA
[1]chiranjit.ju@gmail.com, [2]hirani@mech.iitd.ac.in

Abstract: - MR brake is an electro-mechanical system consists of rotary disk immersed in a MR fluid and surrounded by electromagnet. The braking torque exerted by MR fluid largely depends on geometry and structure of rotary disks and stationary housing. To analyze the various arrangements of MR brake, an APDL code was developed and same has been detailed in the present paper. Based on the braking torque values, the best configuration of MR brake has been recommended.

Key-Words: - MR fluid, MR brake, Electromagnetic simulation, Finite element analysis

1 Introduction

In magnetorheological brake [1-11] torque applied on rotating disc can be controlled by electric current supplied to the electromagnet. Such brake has advantage over conventional disk brakes in nullifying mechanical wear of rotating disc. It is expected that MR brake will perform smooth, jerk free operation and consume lesser power compared to eddy current or magnetic hysteresis brakes.

The control on the shear stress (between zero to τmax) of MR fluid [12-13] is achieved by regulating the magnitude and direction of the magnetic field. The field density is a function of permeability and saturation of materials through which magnetic field passes, brake geometry, number of turns in electromagnetic coil, and current supplied to electromagnetic coil [1-11], [14-16]. The four main parts of the magnetorheological brake are rotor, housing i.e. stator, coil and MR fluids. In the present study, various arrangements of rotor, stator and coil have been analyzed using finite element software. In these brake arrangements, MRF 241ES was considered as MR fluid. The coil, consisting of 1000 turns of AWG 25 copper wire, was supplied the maximum current of 2.5A.

2 Configurations of Magnetorheological Brake

Six possible arrangements, depicted in figure 1, have been analyzed. For simplicity, axi-symmetric shapes of brake elements have been considered.

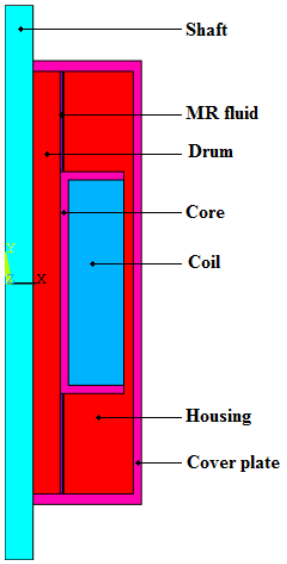

(a) Configuration 1: Drum type MR brake

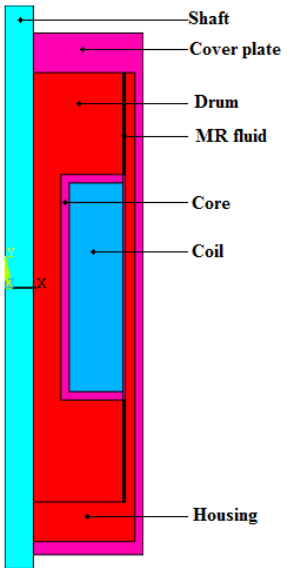

(b) Configuration 2: Inverted Drum MR brake

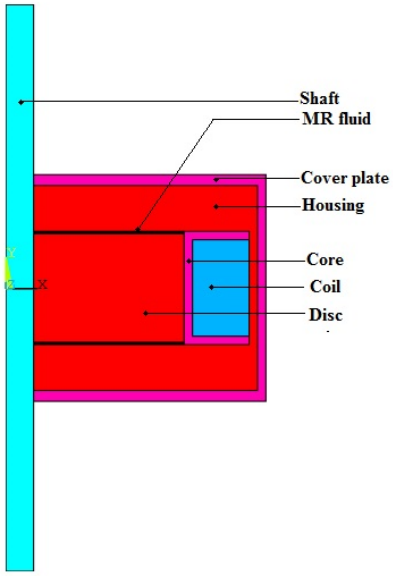

(c) Configuration 3: Disc type MR brake

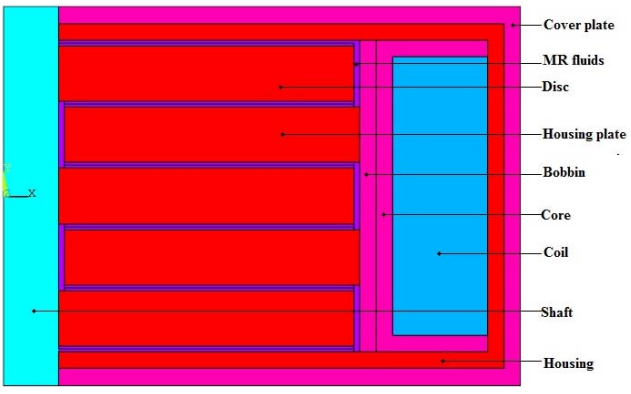

(d) Configuration 4: Multi Discs MR brake

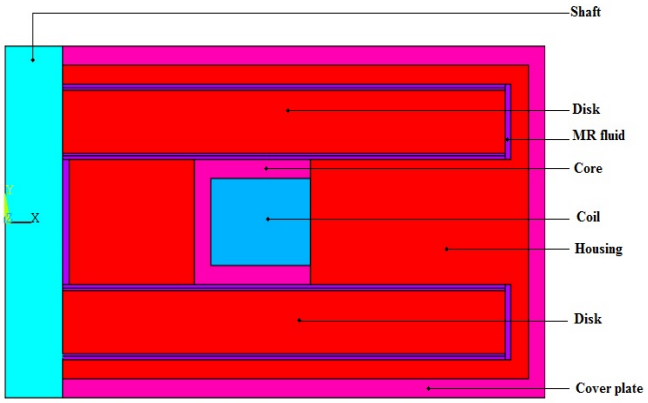

(e) Configuration 5: Multi Discs MR brake considering coil inside

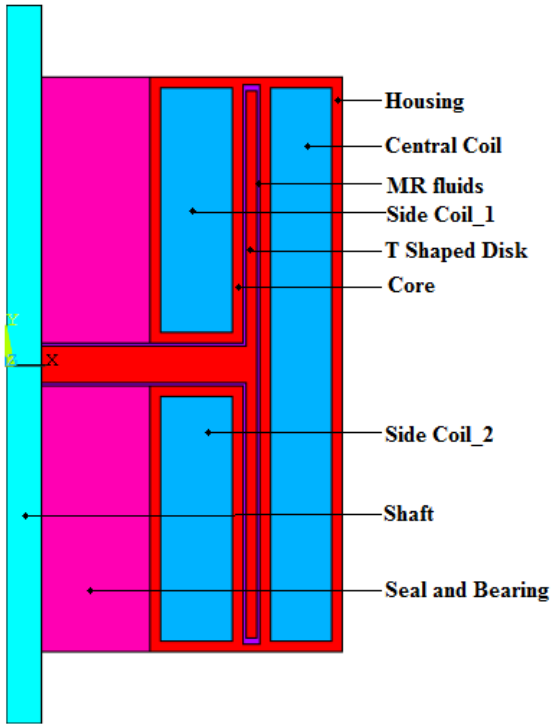

(f) Configuration 6: T shaped Disc MR brake

Fig.1 2-D Axisymmetric MR Brake in ANSYS

In Figure 1 (a) an axi-symmetric view of single disk MR brake has been shown. In this configuration it is assumed that rotating disk is mounted on the shaft with interference-fit and for FEA the shaft and rotating disk can be treated as a single component. Figure 1(b) is similar to Figure 1(a) except the changes in the brake-width and the coil area dimensions. In Figure 1 (c) additional electromagnetic coil pocketed in the housing has been shown. Figure 1 (d) illustrates a 2-D view of multi plate rotating disk attached to shaft and MR fluid around the rotating plates. Here brake pads and housing are stationary members. Three electromagnetic coils are shown in the figure 1(f).

Table1: Nomenclature used in Magnetic Analysis

Symbols	Meaning
BSUM	Magnetic Flux Density or Magnetic Induction
JS	Current Density
B	Vector Magnetic Flux Density
N	Numbers of turns of wires
I	Current
M	Permeability of material used in the Model

In ANSYS, a static (DC) current is provided as input in the form of current density (current over the area of the coil).

$$JS = \frac{(NI)}{A} \tag{1}$$

For given current density, one can determine the magnetic flux density at the rotary disk, MR fluid and the housing. Table 1 lists the magnetic terms used in the present electromagnetic study of MR brake.

To mesh the geometry of MR brake, shown in Figure 1, 2-D quadrilateral Coupled-Field-Solid elements, PLANE 13 were selected. The PLANE 13 element contains four nodes and four degrees of freedom per node. The KEYOPT (3) option was selected to use axisymmetric simulation. The PLANE 13 element can be assigned nonlinear magnetic (B-H curves) properties. SI units were set using the EMUNIT command. The value of μ_0(free-space permeability) was kept equal to $4\pi * 10^{-7}$henries/meter. In ANSYS, the components of magnetic flux density along the x and y axes are expressed as B_x and B_y respectively. The term $B_{Sum}$is defined by

$$B_{sum} = \sqrt{\left(B_x^2 + B_y^2\right)} \tag{2}$$

The values of relative permeability assigned to materials of MR brake components are listed in Table 2.

In the analysis, zero leakage from the housing to the environment was assumed. To impose this condition, constraint of parallel direction of the magnetic flux on boundaries of housing (AZ=0) was used. By default, ANSYS uses the flux to be normal to all exterior faces. 2D magnetic static analysis (using MAGSOLV command) was performed to find the distribution of magnetic flux within the brake housing. To incorporate nonlinear B-H curve, nonlinear analysis (using NSUBST) was carried out. As nonlinear electromagnetic analysis proceeds, ANSYS computes convergence norms with corresponding convergence criteria in each equilibrium iteration. Convergence checking based on magnetic flux density and its tolerance was considered. In the analysis, magnetic flux equal to 1.2 and the tolerance equal to 0.01 were selected, which means the convergence criterion for magnetic flux was kept as 0.012.

Table2: Relative permeability of materials used in MR brake

Parts	Material	Relative Permeability
Shaft	Stainless steel	1
Rotor plate	Low carbon steel	100
Housing	Low carbon steel	100
Seals	Natural Rubber	1
Bearings	Stainless steel	1
MR fluid used	MRF 241 ES	8

Figure 2 shows the flux lines of constant AZ (or constant radius-times-AZ for axisymmetric problems) for all four configurations.

It shows that 2 D flux lines complete the path in the MR brake and cross the MR fluid gaps for all configurations of MR brake. However, to justify the magnetic flux for different configurations, the magnetic flux density plots using nodal solution have been plotted in Figure 3.

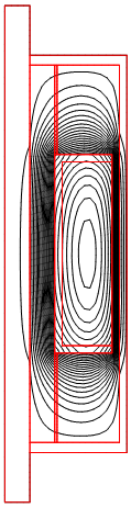

(a) Configuration 1: Drum type MR brake

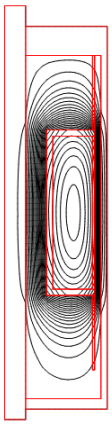

(b) Configuration 2: Inverted Drum type MR brake

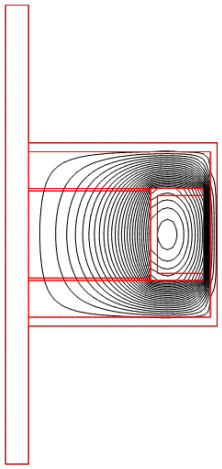

(c) Configuration 3: Disc type MR brake

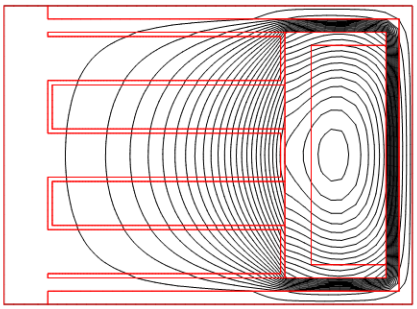

(d) Configuration 4: Multi Discs MR brake

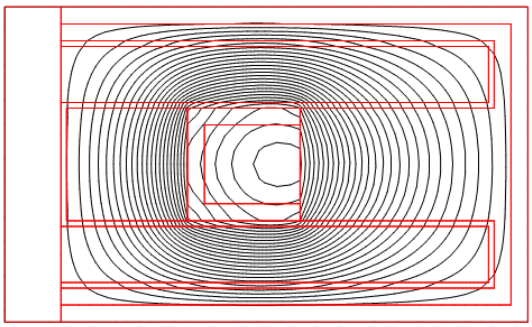

(e) Configuration 5: Multi Discs MR brake considering coil inside

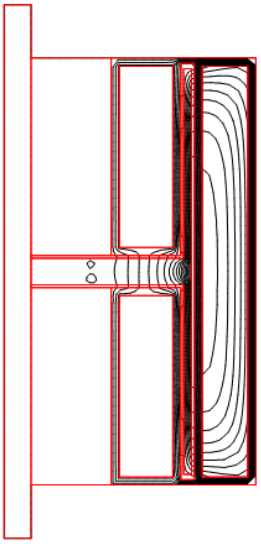

(f) Configuration 6: T shaped Disc MR brake

Fig.22-D Flux Lines around the electrical coil

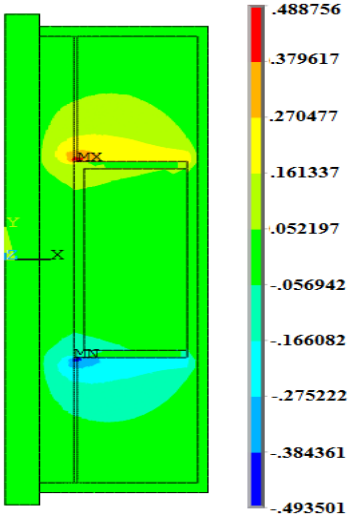

(a) Configuration 1: Drum type MR brake (BX Plot)

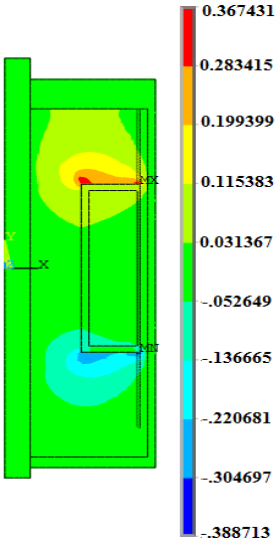

(b) Configuration 2: Inverted Drum type MR brake (BX Plot)

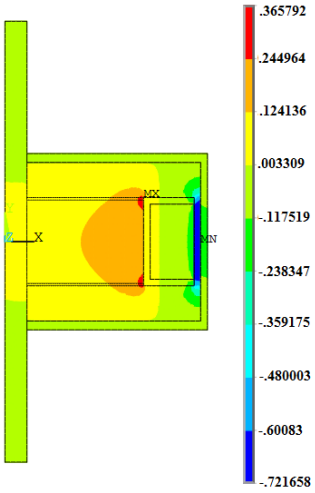

(c) Configuration 3: Disc type MR brake (BY Plot)

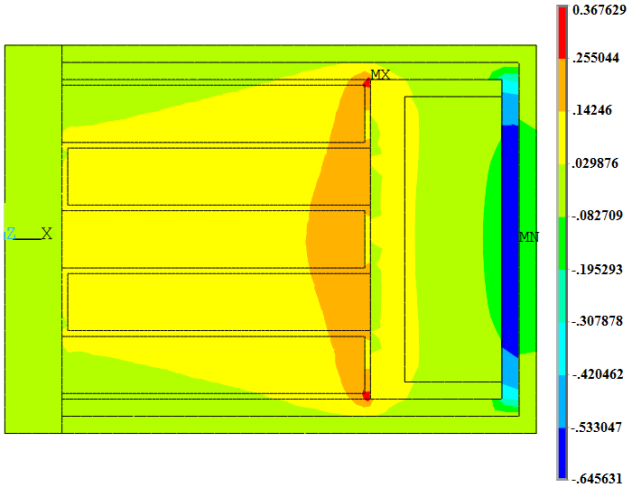

(d) Configuration 4: Multi Disk MR brake (BY Plot)

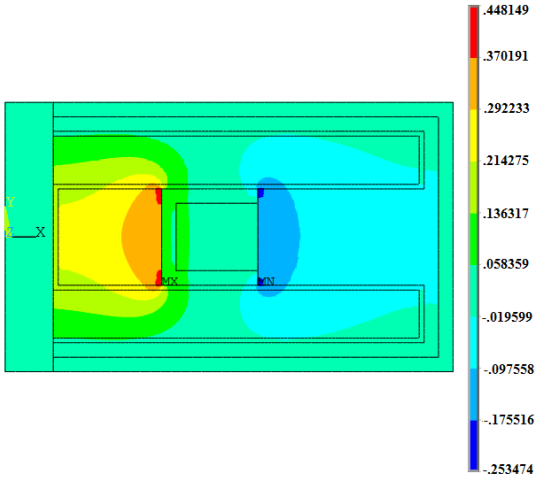

(e) Configuration 5: Multi Disk MR brake considering coil inside (BY Plot)

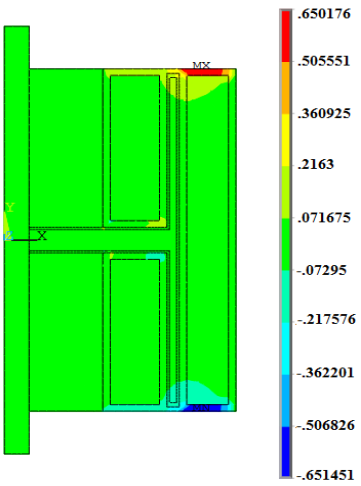

(BX Plot)

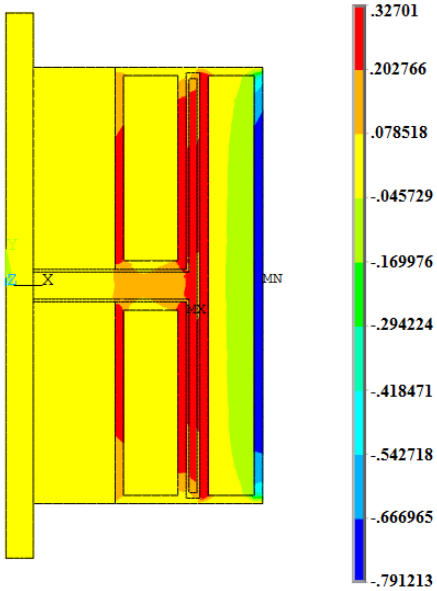

(BY Plot)

(f) Configuration 6: T shaped Disc MR brake

Fig. 3 Nodal Solution-Magnetic Flux Density (B), Tesla

This finite element analysis concludes that magnetic flux density is a function of radius of rotary disk. To estimate the braking torque of MR brake, finite analysis coding (APDL code) was developed.

3 Estimation of braking torque using finite element analysis

The braking torque equations of six different configurations are in the following.

Configuration 1:

$$T = 4\int_{w_1}^{w_2} \pi(r_2 - r_1)h\left(\tau_{yd} + \eta.\frac{\omega.w}{h}\right).dw \quad (1)$$

Configuration 2:

$$T = 4\int_{w_1}^{w_2} \pi(r_2 - r_1)h\left(\tau_{yd} + \eta.\frac{\omega.w}{h}\right).dw \quad (2)$$

Configuration 3:

$$T = \int_{r_1}^{r_2} 4\pi r^2\left(\tau_{yd} + \eta.\frac{\omega.r}{h}\right).dr \quad (3)$$

Configuration 4:

$$T = \int_{r_1}^{r_2} 4n\pi r^2\left(\tau_{yd} + \eta.\frac{\omega.r}{h}\right).dr \quad (4)$$

Configuration 5:

$$T = \int_{r_1}^{r_2} 4n\pi r^2\left(\tau_{yd} + \eta.\frac{\omega.r}{h}\right).dr \quad (5)$$

Configuration 6:

$$T = 4\int_{r_1}^{r_2} \pi r^2\left(\tau_{yd} + \eta.\frac{\omega r}{h}\right).dr + 4\int_{w_1}^{w_2} \pi(r_2 - r_1)h\left(\tau_{yd} + \eta.\frac{\omega w}{h}\right).dw$$
$$+ 2\int_{-w_2}^{w_2} \pi(r_2 - r_1)h\left(\tau_{yd} + \eta.\frac{\omega w}{h}\right).dw \quad (6)$$

Where, r_1 and r_2 are the inner and outer radius of the disk, h is MR fluid gap and $w_1$and $w_2$are the inner and outer disk width. η is the viscosity of carrier fluid, ω is the rotational speed, τ_{yd} is the yield stress of MR fluids. The yield stresses as a function of magnetic field at various nodes of the brake were obtained from the 2-D axisymmetric analyses of all six configurations of MR brake shown in figure 1.

Figure 4 shows the braking torque for six different configurations. It shows the multidisc MR brake gives more braking torque compared to the other MR brake configurations. Hence for the same volume space, multidisc MR brake configuration is a good design.

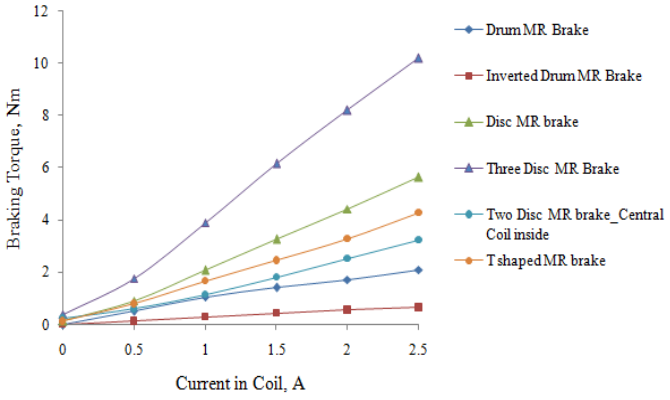

Fig.4 Braking torque of different configurations of MR brake

4 Conclusion

The configurations of MR brake have been analyzed. The following conclusions can be made from the present research work.

- 2 D flux lines complete the path in the MR brake and cross the MR fluid gaps for all configurations of MR brake.
- T shaped MR brake produced the maximum magnetic field due to the three electromagnets.
- The multi-disc MR brake produces more braking torque among the different configurations of MR brake considering same volume space.

References:

[1] C. Sarkar and H. Hirani, Theoretical and experimental studies on a magnetorheological brake operating under compression plus shear mode, *Smart Materials and Structures*, Vol. 22, Art. No. 115032, 2013, 12 pp.

[2] C. Sarkar and H. Hirani, Synthesis and characterization of antifriction magnetorheological fluids for brake, *Defence Science Journal*, Vol. 63 No. 3, 2013, pp. 408-412.

[3] C. Sarkar and H. Hirani, Design of a squeeze film magnetorheological brake considering compression enhanced shear yield stress of magnetorheologicalfluid, *Journal of Physics: Conference Series*, Vol. 412 No. 1, Art. No. 012045, 2013, 12 pp.

[4] C. Sarkar and H. Hirani, Effect of particle size on shear stress of magnetorheological fluids, *Smart Science,* Vol. 3 No. 2, 2015, pp 65-73.

[5] C. Sarkar and H. Hirani, Synthesis and characterization of nano silver particle based magnetorheological fluids for brake, *Defence Science Journal*, Vol. 65 No. 3, 2015, pp. 252-258.

[6] C. Sarkar and H. Hirani, Development of magnetorheological brake with slotted disc, *Proc. IMechE, Part D: Journal of Automobile Engineering*, DOI: 10.1177/0954407015574204, 2015, pp 1-18.

[7] V. K. Sukhwani, V. Lakshmi and H. Hirani, Performance evaluation of MR brake: an experimental study, *Indian Journal of Tribology*, 2006, pp. 67-52.

[8] V. K. Sukhwani and H. Hirani, A comparative study of magnetorheological-fluid-brake and magnetorheological-grease-brake, *Tribology Online*, Vol. 3 No. 1, 2008, pp. 31-35.

[9] V. K. Sukhwani and H. Hirani, Design, development and performance evaluation of high speed MR brake, *Proc. Institute Mech. Engineers., Part L: Journal of Materials: Design and Applications*, Vol. 222 No. 1, 2008, pp.73-82.

[10] V. K. Sukhwani, H. Hirani and T. Singh, Performance evaluation of a magnetorheological grease brake', *Greasetech India*, Vol. 9, 2009, pp. 5-11.

[11] S. Gupta and H. Hirani, Optimization of magnetorheological brake, *ASME/STLE 2011 International Joint Tribology Conference*, Los Angeles, California, 2011, pp 405-406.

[12] J. M. Ginder and L. C. Davis, Shear stresses in magnetorheological fluids: role of magnetic saturation, *Applied Physics Letters*, Vol. 65 No. 26, 1994, pp. 3410-3412.

[13] V. K. Sukhwani and H. Hirani, Synthesis and characterization of low cost magnetorheological (MR) fluids, *The 14th International Symposium on: Smart Structures and Materials & Nondestructive Evaluation and Health Monitoring*, San Diego, USA, 2007, Article no. 65262R.

[14] H. Hirani and C. S. Manjunatha, Performance evaluation of magnetorheological fluid variable valve, *Proc. of the Institution of Mechanical Engineers, Part D: Journal of Automobile Engineering*, Vol. 221 No. 1, 2007, pp. 83-93.

[15] V. K. Sukhwani, H. Hirani and T. Singh, Synthesis of magnetorheological grease, *Greasetech India*, 2007.

[16] V. K. Sukhwani, H. Hirani and T. Singh, Synthesis and performance evaluation of MR grease, *NLGI Spokesman*, 71, 2008.